



**HAL**  
open science

# Random phylogenies and the distribution of branching times

Emmanuel Paradis

► **To cite this version:**

Emmanuel Paradis. Random phylogenies and the distribution of branching times. *Journal of Theoretical Biology*, 2015, 387, pp.39 - 45. 10.1016/j.jtbi.2015.09.005 . hal-01821944

**HAL Id: hal-01821944**

**<https://hal.umontpellier.fr/hal-01821944>**

Submitted on 23 Jun 2018

**HAL** is a multi-disciplinary open access archive for the deposit and dissemination of scientific research documents, whether they are published or not. The documents may come from teaching and research institutions in France or abroad, or from public or private research centers.

L'archive ouverte pluridisciplinaire **HAL**, est destinée au dépôt et à la diffusion de documents scientifiques de niveau recherche, publiés ou non, émanant des établissements d'enseignement et de recherche français ou étrangers, des laboratoires publics ou privés.

# Random phylogenies and the distribution of branching times

Emmanuel Paradis

*Institut des Sciences de l'Évolution, Université Montpellier – CNRS – IRD – EPHE, CC 064, Place Eugène Bataillon,  
F-34095 Montpellier cédex 05, France*

---

## Abstract

Phylogenetic trees reconstructed without fossils have become an important source of information to study evolutionary processes. A widely used method to describe patterns of phylogenetic diversification is known as the lineages-through-time (LTT) plot. Recently, it has been shown that it is possible to predict the distribution of the branching times of a phylogeny, thus making possible to derive a theoretical LTT curve conditioned on diversification parameters. Here, I review some aspects related to this prediction showing how to derive it for any time-dependent model of diversification, as well as calculating a prediction interval around a theoretical LTT curve. The accuracy of the prediction interval was assessed with simulations using fixed or random tree sizes under constant-rate models as well as two models of time-dependent diversification. The prediction intervals were relatively narrower and more accurate for larger trees. The features of this approach are discussed as well as its potential applications.

*Keywords:* diversity, extinction, LTT plot, speciation

---

Tel: +33 (0) 4 67 14 46 85

Fax: +33 (0) 4 67 14 36 14

E-mail: Emmanuel.Paradis@ird.fr

## 1. Introduction

Biological diversity on Earth is the result of several physical, chemical, and biological forces which affect the rates of species origination and extinction. The investigation of evolutionary diversification with phylogenetic trees has received a lot of attention during the last two decades (see recent reviews in Pennell and Harmon, 2013; Morlon, 2014). In particular, a wide range of methods have been developed for the statistical analysis of phylogenies in order to estimate speciation and extinction parameters or to test hypotheses about their variation through time or among different lineages. One popular approach is a graphical method known as the lineage-through time (LTT) plot (Nee et al., 1992). This method requires a dated phylogenetic tree (also known as chronogram) from which the dates of divergence are computed. A plot of the increase in the number of lineages (on the  $y$ -axis) with respect to time (on the  $x$ -axis) is then done to realise the LTT plot. The  $y$ -axis can be log-transformed if, for instance, the increase in the number of lineages is very strong close to present, so that the structure of the curve back in the past may be more visible. The initial motivation behind this method was to find a relationship between the shape of the curve displayed by the LTT plot and the temporal variation (or lack of) in the speciation and extinction rates of the lineage under study. Two approaches to this end can be found in the literature. The first one is based on deriving explicit equations of the distribution of the branching times of a tree with respect to the diversification parameters (e.g., Stadler, 2008; Paradis, 2011; Hallinan, 2012). The second one, which has enjoyed some success in the recent literature, is to simulate many trees under a given model of diversification and then derive a null distribution of the LTT plot (e.g., Crisp and Cook, 2009; Pie and Tschá, 2009; Fordyce, 2010; Lorén et al., 2014).

Recently, Lambert and Stadler (2013) investigated in details general macroevolutionary models of speciation and extinction. An important result from this study is that under a homogeneous model of diversification, the distribution of branching times depends only on the rates of speciation and extinction. Therefore, the LTT plot of a phylogenetic tree completely summarises the information required to estimate these rates under the assumption of homogeneity (i.e., speciation and extinction rates are the same for all species at a given time

though these parameters may vary through time) and the assumption that both rates are not  
30 correlated. On the other hand, remarkable progress has been accomplished on the simulation of  
phylogenetic trees under various diversification models with specified or random numbers of  
species (Paradis, 2011; Stadler, 2011; Höhna, 2013). An issue that remains open concerns the  
33 links between these different methods and approaches, particularly whether explicit equations  
and simulations of phylogenetic trees lead to similar prediction of branching times distribution.  
Another question is about the effect of simulating a phylogeny with a specified number of species  
36 on the distribution of branching times. Finally, the nature of the variability around the predicted  
distribution of branching times has not yet been assessed.

In the present paper, I review the question of predicting the distribution of branching times of  
39 a phylogeny given a model of temporal variation in speciation and extinction rates. Further  
elaborating on the work presented in Paradis (2011), I show how the calculations can be improved  
and applied to any model of time-dependent diversification. I then discuss how to derive a  
42 prediction interval around the theoretical LTT curve. I also review the methods for simulating  
phylogenetic trees from speciation–extinction models, and discuss the relationships among the  
different approaches. Using stochastic simulations, it is shown that the prediction interval of the  
45 LTT plot can be accurate in different settings of diversification parameters and tree sizes.

## 2. Methods

### 2.1. Speciation–extinction models and the distribution of branching times

48 Throughout this paper, we consider a dated (i.e., ultrametric) phylogenetic tree with  $N$  species.  
We assume that this tree is rooted and fully dichotomous; consequently, it has  $N - 1$  ( $= m$ )  
internal nodes. The branching times, measured from the root, are denoted  $t_1, \dots, t_m$ . By  
51 convention in this paper, the root is the origin of the time scale, so that  $t_1 = 0$ , and the present is  
denoted  $T$ .

Birth–death models have been widely used to analyse or simulate the diversification of  
54 clades. The basic assumption of these models is that each species is continuously exposed to  
speciation and extinction. The rates at which these events happen may vary through time. In such

a time-dependent birth–death model, the probability that a species undergo speciation follows a  
 57 function denoted  $\lambda(t)$ , and similarly for the probability of extinction  $\mu(t)$ . This formulation  
 implies no lineage-specific variation: at a given time, all species have the same probabilities of  
 speciation and extinction (i.e., the assumption of homogeneity). In order to derive the predicted  
 60 LTT curve under a time-dependent birth–death model, we use the probability that a lineage,  
 originating from a single species at time  $t$ , is not extinct at time  $T$  (Kendall, 1948):

$$\Pr(t, n_T \geq 1) = \frac{e^{-\rho(t,T)}}{W(t)}, \quad (1)$$

where  $n_T$  is the number of living species in the lineage at time  $T$ , and with the function  $\rho$  defined  
 63 as:

$$\rho(t, T) = \int_t^T \mu(u) - \lambda(u) du,$$

and:

$$W(t) = e^{-\rho(t,T)} \left[ 1 + \int_t^T e^{\rho(t,u)} \mu(u) du \right].$$

We note that in eq. 1,  $t$  and  $T$  are given fixed values; only  $n_T$  is a random variable.

66 We can now derive the distribution of branching times from the phylogeny. The probability of  
 observing a branching event in a phylogeny, denoted as  $\pi(t)$ , is given by the probability that two  
 lineages originating at time  $t$  survive until present multiplied by the probability of a speciation  
 69 event at  $t$ . The latter probability is given by the product of the speciation probability at  $t$ ,  $\lambda(t)$ ,  
 with the number of species living at this time. Obviously, we do not know the latter but we can  
 substitute it by its expectation:  $\mathbb{E}(n_t) = e^{-\rho(0,t)}$ . Consequently, we have:

$$\pi(t) = \Pr^2(t, n_T \geq 1) \mathbb{E}(n_t) \lambda(t). \quad (2)$$

72 This density gives the relative probabilities of a branching time on the interval  $0 < t < T$ , but this  
 is not a probability density because this function does not integrate (since  $t$  is continuous) to one.

We rescale this equation with respect to  $t$  on the interval  $[0, T]$  to obtain a cumulative density  
 75 function (CDF) of the branching times:

$$\mathcal{F}(t) = \frac{\int_0^t \pi(u) du}{\int_0^T \pi(u) du}. \quad (3)$$

This equation is used to derive the predicted curve of the LTT plot with given functions  $\lambda(t)$  and  
 $\mu(t)$  (Paradis, 2011).  $\mathcal{F}(t)$  is an increasing function with increasing  $t$ , and we have  $\mathcal{F}(0) = 0$  and  
 78  $\mathcal{F}(T) = 1$ . Höhna (2013) derived an equation which is close but different from eq. 2 above.  
 However, it can be shown that both forms are equivalent (see Appendix A).

As one can see from the above formulae, the calculations involved in computing  $\mathcal{F}(t)$  are  
 81 quite heavy with several integrations which, in general, cannot be solved analytically (a trivial  
 exception is the case with  $\lambda$  and  $\mu$  constant). In practice, standard numerical methods for  
 integration can be used but they are usually slow. Hallinan (2012) found an interesting solution to  
 84 this problem: if one assumes that  $\lambda(t)$  and  $\mu(t)$  are constant across some time intervals (i.e., they  
 vary following some step functions), then eq. 1 can be calculated easily. This is an interesting  
 solution because the assumption that speciation and extinction rates are constant over some short  
 87 time periods (e.g., a few thousand years) may be reasonable on a macroevolutionary scale  
 (several million years).

Here I develop some improvements on the computation of the above equations that make the  
 90 calculation of  $\mathcal{F}(t)$  faster for any function  $\lambda(t)$  and  $\mu(t)$ . First, we note that eq. 1 simplifies to:

$$\Pr(t, n_T \geq 1) = \left[ 1 + \int_t^T e^{\rho(t,u)} \mu(u) du \right]^{-1}.$$

We then log-transform eq. 2:

$$\ln \pi(t) = -2 \ln \left[ 1 + \int_t^T e^{\rho(t,u)} \mu(u) du \right] - \rho(0, t) + \ln \lambda(t).$$

Working on a logarithmic scale is less likely to inflate computing errors since we work here with  
 93 sums instead of products. Note that if the antiderivates of  $\lambda(t)$  and of  $\mu(t)$  can be found, say  $\Lambda(t)$

and  $M(t)$ , then  $\rho(t, u)$  can be computed directly:

$$\rho(t, u) = M(u) - \Lambda(u) - M(t) + \Lambda(t).$$

For instance, if both follow some step functions, as assumed in Hallinan (2012), then these  
96 antiderivates are calculated simply with rectangle areas. The two remaining difficulties are the  
integral of  $e^{\rho(t, u)}\mu(u)$  and the one of  $\pi(t)$ . To compute them efficiently, the following strategy has  
been adopted. The function to be integrated is first evaluated on a sufficiently large number of  
99 points which are defined so that two neighbouring points are close enough so the area under the  
curve can be approximated with a rectangle. For instance (where  $\delta$  is a small value):

$$\int_x^{x+\delta} \pi(u) du \approx \pi(x + \delta/2) \times \delta.$$

This is a standard step in computing an integral with an unknown antiderivative and is called the  
102 midpoint method. The integral between 0 and  $t$  is then calculated with the sum of all the rectangle  
areas between these two values. We have to be careful that the error generated by the midpoint  
method, which may be negligible for a single small interval, will tend to accumulate when  
105 summing over many such intervals. A solution is to use Simpson's rule which is defined by:

$$\int_x^{x+\delta} \pi(u) du \approx \frac{\pi(x) + 4\pi(x + \delta/2) + \pi(x + \delta)}{6} \times \delta.$$

Over a wider interval made of many elementary intervals, the values of all left-, mid-, and  
right-points of each elementary interval are summed using the same coefficients as above (1, 4,  
108 and 1). In the framework of the present application, it was found that defining 500 elementary  
intervals was enough, so that it is needed to calculate 999 values of  $\pi(t)$ . Both integrals in eq. 3  
are then calculated with Simpson's rule (the denominator being calculated over all elementary  
111 intervals).

## 2.2. The lineage-through time plot and its prediction interval

Simulations show clearly that the distribution of branching times is highly variable even with the  
114 same parameter values. So it is desirable to predict the variability around the expected LTT plot  
in the same way than prediction bands are derived in statistical practice (Liu et al., 2008). We use  
here an approach introduced by Hallinan (2012) whose rationale is as follows: consider a point in  
117 time, say  $\tau$ , and let us write  $p = \mathcal{F}(\tau)$ . Consider now a branching time  $t$  taken at random in a tree  
generated with the same parameters used to compute  $\mathcal{F}$ . Then, by the definition of a CDF, the  
event  $t \leq \tau$  follows a Bernoulli distribution with probability  $p$ . We can thus derive upper and  
120 lower bounds for the CDF of branching times by calculating the quantiles of the number of  
observed branching times for each value of  $t$ . Suppose we observe  $n$  branching times, then the  
number of those smaller than or equal to  $\tau$  follows a binomial distribution with parameters  $n$  and  
123  $p$ . It is therefore possible to calculate a 95% prediction interval of this distribution using the  
quantiles of the binomial distribution at the probabilities 0.025 and 0.975. In practice, these  
bounds are calculated at a number of points in the interval  $[0, T]$  (every 0.1 time unit in this  
126 paper).

## 2.3. Simulating speciation–extinction trees

Simulating evolutionary data has become an important endeavour in data analysis with the  
129 constant development of Monte Carlo or Bayesian approaches. There is a long history of the  
simulation of trees with different purposes (see Paradis, 2014, for a brief overview). The  
simulation of speciation–extinction (or birth–death) trees is only a subset of these methods. Two  
132 broad categories of methods to simulate speciation–extinction trees can be defined: the  
homogeneous methods which are continuous in time, and the heterogeneous methods which can  
model any kind of variation in speciation and extinction rates (in relation to species biological  
135 traits, environment, climate, . . .) I consider only the former category here, and distinguish three  
approaches to this:

1. Starting from a single species, evolution is simulated forward in time. The times of  
138 speciation and extinction events are simulated with time-to-event (or waiting time)



formulae (Paradis, 2011).

2. Starting from present and a given number of species, evolution is simulated backward in  
141 time. The times of speciation and extinction events are simulated with a coalescent  
approach (Stadler, 2011).
3. Branching times are sampled randomly from the expected distribution described in the  
144 previous section. The topology of the tree is built by random successive agglomeration of  
species.

There can be many variants around these broad lines. For instance, the simulation can start  
147 from a (root) node instead of a single species. Another variation is to record or not the extinction  
events: if one is only interested in ultrametric trees (i.e., without fossils) then the extinct lineages  
may be simply discarded to speed-up calculations (Paradis, 2011).

150 These three approaches share in common that they simulate branch lengths in continuous  
time making comparisons easier because the outputs do not depend on the definition of arbitrary  
time steps. The first approach makes possible to simulate a tree with a fixed value of  $T$  ( $N$  is  
153 always random), while the second one can simulate trees with fixed  $N$  ( $T$  is random), and the  
third one can do simulations with both  $T$  and  $N$  fixed. The first approach has been used in earlier  
works to simulate trees with  $N$  fixed; however, Hartmann et al. (2010) demonstrated that this  
156 approach results in biased simulated trees and presented a method to remedy this problem.

Various implementations of these approaches are available in different computer programs.  
The first approach is implemented in *ape* (Paradis et al., 2004) which provides two algorithms  
159 (depending on whether extinct lineages are recorded or not) which simulate trees with any  
time-dependent variation in  $\lambda$  and  $\mu$  (these parameters may be constant). The second approach is  
implemented in *TreeSim* (Stadler, 2014) which can simulate trees with constant  $\lambda$  and  $\mu$  and the  
162 possibility to include random sampling of species as well as episodic (mass) extinctions. In order  
to complete this, I implemented in *ape* the possibility to simulate a tree with  $N$  fixed and any kind  
of time-dependent variation in both  $\lambda$  and  $\mu$  (which still can be constant). This uses a slightly  
165 modified version of the algorithm given in Stadler (2011). The difference is in the way waiting  
times are generated (step 2 of the original algorithm), specifically, the formula used to generate a

random time  $x$  starting from time  $t$  is here:

$$n_t [\lambda(t) + \mu(t)] \exp \left[ -n_t \int_x^t \lambda(u) + \mu(u) du \right].$$

168 We keep in mind that in the framework used in this paper the time scale goes from past to present, so  $x < t$  since the algorithm goes backward in time. If  $\lambda$  and  $\mu$  are constant, the above formula simplifies to  $n_t(\lambda + \mu)e^{n_t(\lambda + \mu)(t-x)}$  which is the probability density function of an  
171 exponential distribution with rate  $n_t(\lambda + \mu)$ , thus making possible to use efficient random number generators from common statistical software.

Finally, the third approach is implemented in TESS which can simulate trees with any  
174 time-dependent model (Höhna, 2013).

#### 2.4. Simulation study

A simulation study was conducted in order to assess the effect of tree size and diversification  
177 parameters on the predictions of the distribution of branching times. Two of the above simulation algorithms were used to generate phylogenetic trees. The first one is described in Paradis (2011) and simulates a tree in continuous time where  $\lambda$  and  $\mu$  are allowed to vary with time under any  
180 user-specified model. This is a time-forward algorithm where  $T$  is fixed and  $N$  is variable (first approach of the previous section). The second algorithm is due to Stadler (2011) and simulates trees in continuous time using a time-backward method with  $N$  fixed (second approach of the  
183 previous section). Both algorithms require as input the values of the parameters  $\lambda$  and  $\mu$  and are implemented in the R (R Core Team, 2014) packages `ape` and `TreeSim` (Stadler, 2014), respectively. The third approach described in the previous section was not considered here  
186 because it samples branching times directly from the expected LTT curve, so a good agreement between the simulated trees and the predictions should be no surprise.

The predicted LTT plot and its 95% prediction interval were computed for a given set of  
189 parameter values. Ten thousand trees were simulated for each set of parameter values with both algorithms. For each tree, the LTT plot was calculated, and the agreement with the predictions were assessed in two ways. First, the proportion of points falling within the 95% prediction

192 interval was counted. Second, the proportion of points falling above or below the predicted curve  
was also counted. Two sets of simulations were done. In the first set,  $\lambda$  and  $\mu$  were kept constant  
with values given in Table 1. In the second set, two models of temporal variation were  
195 considered: the first one is an early burst model of speciation with decreasing  $\lambda$  through time and  
constant  $\mu$  (Fig. 2a); the second one is a model of increasing extinction in recent time and  
constant  $\lambda$  (Fig. 3a).

### 198 3. Results

The proportion of points of the LTT plots falling within the prediction intervals depended mainly  
on the size of the tree (Table 1). For trees simulated with  $N = 10$ , about 69% of the points fell  
201 within the prediction intervals for all values of  $\lambda$  and  $\mu$ . This rose to about 90% for  $N = 50$ , and  
94% for  $N = 200$ . For  $N = 1000$ , this percentage was slightly larger when  $\lambda = 0.1$  (94%) than  
when  $\lambda = 0.2$  (93%). For trees generated with a random value of  $N$ , the percentage of points  
204 outside the prediction interval was related to the value of the difference  $\lambda - \mu$ : when this  
difference was large, the percentage was above 93% whereas it was below 70% for the smallest  
values.

207 A similar pattern emerged from the proportion of points above the predicted curve (Table 2).  
Except for trees simulated with  $N \leq 20$ , the points were as likely to be above than below the  
predicted LTT curve. The same result was observed with random  $N$ . Figure 1 shows the predicted  
210 LTT plots under two sets of parameters:  $\lambda = 0.1, \mu = 0$ , and  $\lambda = 0.3, \mu = 0.2$ . The expected  
number of species is the same in both cases since the difference  $\lambda - \mu$  is the same. As expected,  
the 95% prediction intervals depended on the size of the tree (shown for  $N = 20$  and  $N = 200$ ).

213 Figure 2a shows the modelled rates  $\lambda$  and  $\mu$  under the scenario of early burst together with the  
predicted LTT curve. Figure 2b shows the LTT plot from a tree simulated with this model. By  
contrast to the cases with constant speciation and extinction rates, the proportion of points of the  
216 LTT plots falling within the prediction intervals varied little with respect to  $N$  and was around  
90% (Table 3). The proportion of points below the predicted LTT curve was around 35% and did  
not vary much with tree size except when  $N$  was random where it was above 50% (Table 4).

219 Figure 3a shows the modelled rates  $\lambda$  and  $\mu$  under the scenario of increasing extinction  
together with the predicted LTT curve. Figure 3b shows the LTT plot from a tree simulated with  
this model. With this scenario, the proportion of points of the LTT plots within the prediction  
222 intervals decreased slightly with increasing tree size ranging from around 92% to around 82%  
(Table 3). Similarly to the previous scenario, most of these points were below the predicted curve  
except when  $N$  was random (Table 4).

#### 225 4. Discussion

The LTT plot is one of the most widely used methods to assess diversification from dated  
phylogenies. Its simplicity to run and its ability to display temporal phylogenetic patterns make it  
228 an attractive tool for evolutionists studying many groups. This method has some limitations,  
particularly some are intrinsic to the analysis of reconstructed phylogenies which ignore fossils  
(see review in Morlon, 2014). In spite of these limitations, which are now well-known, the LTT  
231 plot has proven to be a valuable tool for investigating evolutionary diversification from molecular  
phylogenies (e.g., Moreau et al., 2006; Bininda-Emonds et al., 2007; Lorén et al., 2014).

This paper aims to review some recent developments on the analysis of branching times from  
234 phylogenetic trees with a focus on predicting their distribution. It is possible to compute a  
predicted LTT curve as well as a prediction interval around the predicted curve. Some  
improvements to compute this predicted LTT curve are presented above. The prediction interval  
237 is computed with the assumption that the branching times of the phylogeny follow a binomial  
distribution at any given time.

One issue for computing a predicted LTT curve is the justification of the parameter values. In  
240 the examples presented in this paper, these values were taken as fixed and given a priori, because  
the data were simulated so the real diversification parameter values of the phylogenies were  
known. With real data, the situation is different and the parameters must be estimated from the  
243 data. Two applications are possible in this context. First, it is possible to calculate an “empirical”  
confidence interval around the observed LTT plot with the same approach as described above: the  
values of  $p$  would thus be calculated from the observed cumulated proportions of number of

246 lineages. Such a confidence interval is actually “model free” (i.e., they do not require to estimate  
the diversification parameters). The second application is to infer a predicted LTT curve from a  
fitted model and draw it together with the observed LTT plot. For instance, suppose a  
249 constant-parameter birth–death model is fitted to a tree, then the estimated values of  $\lambda$  and  $\mu$  can  
be used to draw a predicted LTT curve and compare it with the actual distribution of branching  
times. Such an approach can help to assess the goodness of the fit of a particular model of  
252 diversification (see also Wollenberg et al., 1996; Paradis, 1998).

The match between the prediction intervals and the simulated trees showed various degrees of  
agreement. For the constant-parameter models, the degree of success of the prediction intervals  
255 was mainly related to the tree size ( $N$ ). With  $N = 1000$ , almost 95% of the points from the LTT  
plots of the simulated trees were within the 95% prediction intervals. When trees were simulated  
with random  $N$ , the precision of the predictions were positively related to the net diversification  
258 rate ( $\lambda - \mu$ ), thus confirming the importance of tree size since trees simulated with a higher  
diversification rate are expected to have larger sizes (since the time of evolution of the simulated  
trees,  $T$ , was kept constant). An interesting result was that, for almost all simulations with  
261 constant parameters, the points of the LTT plots have the same probability to fall above or below  
the predicted LTT curve, with only a slightly higher proportion (*ca.* 0.55) of points below this  
curve for the smaller trees (see Table 2).

264 The success of the predictions was more contrasted when trees were simulated with the  
time-dependent models of diversification. Overall, the proportion of points of the LTT plots  
within the prediction interval was similar to the constant-rate case with similar tree sizes.  
267 However, this proportion did not change much with tree size and did not reach 95% like for the  
constant-rate case. On the other hand, the points tend to be on one side of the predicted LTT curve  
and slightly preferentially above it.

270 Paradis (2011) and Etienne and Rosindell (2012) proposed to fit models of diversification and  
estimate the parameters by minimising the deviation between the observed LTT curve and the  
one predicted from the model using a least squares criterion. It has been shown that this fitting  
273 procedure performs better than fitting the same model by maximum likelihood at least in some

situations (Paradis, 2011). Hallinan (2012) questioned the use of LTT plots as a tool to assess the fit of a diversification model to a phylogenetic tree. The difficulty appears to be the  
276 autocorrelation of the individual points of an LTT plot: successive points tend to be above or below the predicted line as shown by the examples in this paper. However, the simulation results reported here suggest that, when speciation and extinction rates are constant through time, the  
279 points do not statistically tend to be either above or below the predicted line over the complete range of the plot, even within a single LTT plot. This seems to validate the use of a least squares approach to model fitting. On the other hand, when these rates varied through time, the points  
282 tended to be above the predicted LTT curve which may result in biased parameter estimation. This will require further study.

To conclude, the distribution of branching times can be well predicted by the above formula  
285 (eq. 3) when the speciation and extinction rates are constant through time. The predictions are still accurate but less consistent for the time-dependent models considered here, which is a point requiring further study. A prediction interval around the predicted distribution (i.e., the LTT  
288 curve) can be derived and is accurate except for the smallest tree sizes. In spite of being more than two-decade old, the LTT plot is a flexible and very useful graphical tool to display the distribution of branching times, either from phylogenetic trees, or from predictions derived from  
291 speciation–extinction models.

### **Acknowledgements**

I am grateful to Tanja Stadler for clarification about some issues on tree simulation, and to two  
294 anonymous reviewers for their comments. This is publication ISEM 201x-xxx.

### **Appendix A**

Höhna (2013, eq. 8) derived the probability of speciation events in a phylogenetic tree as (using  
297 the notation of the present paper):

$$\pi(t) \propto \Pr(t, n_T = 1)\lambda(t).$$

The probability that a lineage originating at time  $t$  has a single species at time  $T$  used by Höhna is (Kendall, 1948, eq. 16):

$$\Pr(t, n_T = 1) = \frac{e^{-\rho(t,T)}}{W(t)^2}.$$

300 We now develop eq. 2 of the present paper:

$$\begin{aligned} \pi(t) &= \Pr(t, n_T \geq 1)^2 \mathbb{E}(n_t) \lambda(t) \\ &= \left[ \frac{e^{-\rho(t,T)}}{W(t)} \right]^2 e^{-\rho(0,t)} \lambda(t) \\ &= \frac{e^{-\rho(t,T)}}{W(t)^2} e^{-\rho(t,T)} e^{-\rho(0,t)} \lambda(t). \end{aligned}$$

We note that:

$$e^{-\rho(t,T)} e^{-\rho(0,t)} = e^{-\rho(0,T)}.$$

We also note that the fraction is equal to  $\Pr(t, n_T = 1)$ , and reordering the terms in the product  
303 this gives:

$$\pi(t) = \Pr(t, n_T = 1) \lambda(t) e^{-\rho(0,T)},$$

which is identical to Höhna's equation and shows what is the proportionality factor. We note that the latter does not depend on  $t$ , so its value will cancel out in the ratio of integrals in eq. 3 (also in  
306 Höhna, 2013, eq. 9).

## References

- Bininda-Emonds, O. R. P., Cardillo, M., Jones, K. E., MacPhee, R. D. E., Beck, R. M. D.,  
309 Grenyer, R., Price, S. A., Vos, R. A., Gittleman, J. L., Purvis, A., 2007. The delayed rise of present-day mammals. *Nature* 446, 507–512.

- Crisp, M. D., Cook, L. G., 2009. Explosive radiation or cryptic mass extinction? Interpreting  
312 signatures in molecular phylogenies. *Evolution* 63 (9), 2257–2265.
- Etienne, R. S., Rosindell, J., 2012. Prolonging the past counteracts the pull of the present:  
protracted speciation can explain observed slowdowns in diversification. *Syst. Biol.* 61 (2),  
315 204–213.
- Fordyce, J. A., 2010. Interpreting the  $\gamma$  statistic in phylogenetic diversification rate studies: a rate  
decrease does not necessarily indicate an early burst. *PLoS ONE* 5 (7), e11781.
- 318 Hallinan, N., 2012. The generalized time variable reconstructed birth–death process. *J. Theor.*  
*Biol.* 300, 265–276.
- Hartmann, K., Wong, D., Stadler, T., 2010. Sampling trees from evolutionary models. *Syst. Biol.*  
321 59 (4), 465–476.
- Höhna, S., 2013. Fast simulation of reconstructed phylogenies under global time-dependent  
birth–death processes. *Bioinformatics* 29 (11), 1367–1374.
- 324 Kendall, D. G., 1948. On the generalized “birth-and-death” process. *Ann. Math. Stat.* 19, 1–15.
- Lambert, A., Stadler, T., 2013. Birth–death models and coalescent point processes: the shape and  
probability of reconstructed phylogenies. *Theor. Pop. Biol.* 90, 113–128.
- 327 Liu, W., Lin, S., Piegorsch, W. W., 2008. Construction of exact simultaneous confidence bands  
for a simple linear regression model. *Int. Statist. Rev.* 76 (1), 39–57.
- Lorén, J. G., Farfán, M., Fusté, M. C., 2014. Molecular phylogenetics and temporal  
330 diversification in the genus *Aeromonas* based on the sequences of five housekeeping genes.  
*PLoS ONE* 9 (2), e88805.
- Moreau, C. S., Bell, C. D., Vila, R., Archibald, S. B., Pierce, N. E., 2006. Phylogeny of the ants:  
333 diversification in the age of angiosperms. *Science* 312, 101–104.
- Morlon, H., 2014. Phylogenetic approaches for studying diversification. *Ecol. Lett.* 17 (4),  
508–525.
- 336 Nee, S., Mooers, A. Ø., Harvey, P. H., 1992. Tempo and mode of evolution revealed from  
molecular phylogenies. *Proc. Natl. Acad. Sci. USA* 89 (17), 8322–8326.
- Paradis, E., 1998. Testing for constant diversification rates using molecular phylogenies: a



- 339 general approach based on statistical tests for goodness of fit. *Mol. Biol. Evol.* 15 (4), 476–479.
- Paradis, E., 2011. Time-dependent speciation and extinction from phylogenies: a least squares approach. *Evolution* 65 (3), 661–672.
- 342 Paradis, E., 2014. Simulation of phylogenetic data. In: Garamszegi, L. Z. (Ed.), *Modern Phylogenetic Comparative Methods and Their Application in Evolutionary Biology*. Springer-Verlag, Berlin Heidelberg, pp. 335–350.
- 345 Paradis, E., Claude, J., Strimmer, K., 2004. APE: analyses of phylogenetics and evolution in R language. *Bioinformatics* 20 (2), 289–290.
- Pennell, M. W., Harmon, L. J., 2013. An integrative view of phylogenetic comparative methods: 348 connections to population genetics, community ecology, and paleobiology. *Ann. N.Y. Acad. Sci.* 1289, 90–105.
- Pie, M., Tschá, M. K., 2009. The macroevolutionary dynamics of ant diversification. *Evolution* 351 63 (11), 3023–3030.
- R Core Team, 2014. *R: A Language and Environment for Statistical Computing*. R Foundation for Statistical Computing, Vienna, Austria.
- 354 URL <http://www.R-project.org>
- Stadler, T., 2008. Lineages-through-time plots of neutral models for speciation. *Math. Biosci.* 216 (2), 163–171.
- 357 Stadler, T., 2011. Simulating trees with a fixed number of extant species. *Syst. Biol.* 60 (5), 676–684.
- Stadler, T., 2014. *TreeSim: Simulating trees under the birth-death model*. R package version 2.1.
- 360 URL <http://CRAN.R-project.org/package=TreeSim>
- Wollenberg, K., Arnold, J., Avise, J. C., 1996. Recognizing the forest for the trees: testing temporal patterns of cladogenesis using a null model of stochastic diversification. *Mol. Biol.* 363 *Evol.* 13 (6), 833–849.

**Fig. 1.** Lineage-through time plots (grey lines) for ten simulated trees with different values of speciation ( $\lambda$ ) and extinction ( $\mu$ ) rates and tree size ( $N$ ). The thick line shows the predicted LTT distribution, and the dashed lines delimit the 95% prediction intervals. The y-axes are scaled to one. F: cumulative proportions of lineages.

**Fig. 2.** (a) The early burst model of speciation showing the parameters ( $\lambda$  and  $\mu$ ) and the predicted LTT curve. (b) The LTT plot from a phylogeny simulated with this model (black line) and the number of living lineages (grey line) from the same simulation.

**Fig. 3.** (a) A model of increasing extinction in recent time showing the parameters ( $\lambda$  and  $\mu$ ) and the predicted LTT curve. (b) The LTT plot from a phylogeny simulated with this model (black line) and the number of living lineages (grey line) from the same simulation.

Table 1: Proportion of points from the LTT plots falling within the 95% prediction interval. The simulations were replicated 10,000 times. All trees were simulated with  $T = 50$  and  $n_0 = 1$ .  $N$ : number of species in the tree;  $\lambda$ : speciation rate;  $\mu$ : extinction rate.

| $\lambda$ | $\mu$ | $N$   |       |       |       |       |       |        |
|-----------|-------|-------|-------|-------|-------|-------|-------|--------|
|           |       | 10    | 20    | 50    | 100   | 200   | 1000  | random |
| 0.1       | 0     | 0.692 | 0.817 | 0.900 | 0.930 | 0.942 | 0.943 | 0.935  |
|           | 0.05  | 0.691 | 0.818 | 0.900 | 0.927 | 0.939 | 0.945 | 0.847  |
|           | 0.09  | 0.691 | 0.817 | 0.900 | 0.927 | 0.939 | 0.942 | 0.680  |
| 0.2       | 0.1   | 0.690 | 0.817 | 0.899 | 0.926 | 0.937 | 0.931 | 0.933  |
|           | 0.15  | 0.690 | 0.815 | 0.897 | 0.925 | 0.937 | 0.932 | 0.893  |
|           | 0.19  | 0.691 | 0.818 | 0.899 | 0.925 | 0.938 | 0.932 | 0.787  |

Table 2: Proportion of points from the LTT plots falling below the predicted LTT line. See Table 1 for details.

| $\lambda$ | $\mu$ | $N$   |       |       |       |       |       |        |
|-----------|-------|-------|-------|-------|-------|-------|-------|--------|
|           |       | 10    | 20    | 50    | 100   | 200   | 1000  | random |
| 0.1       | 0     | 0.546 | 0.521 | 0.505 | 0.505 | 0.501 | 0.504 | 0.505  |
|           | 0.05  | 0.548 | 0.525 | 0.504 | 0.512 | 0.509 | 0.501 | 0.513  |
|           | 0.09  | 0.553 | 0.525 | 0.515 | 0.512 | 0.501 | 0.507 | 0.550  |
| 0.2       | 0.1   | 0.552 | 0.527 | 0.507 | 0.496 | 0.500 | 0.500 | 0.502  |
|           | 0.15  | 0.551 | 0.522 | 0.510 | 0.506 | 0.500 | 0.499 | 0.516  |
|           | 0.19  | 0.539 | 0.517 | 0.521 | 0.510 | 0.502 | 0.504 | 0.529  |

Table 3: Proportion of points from the LTT plots falling within the 95% prediction interval for two models of time-dependent diversification. The simulations were replicated 10,000 times.  $T$  was random except when  $N$  was random where  $T = 50$  and  $n_0 = 1$ .

| Model             | $N$   |       |       |       |        |
|-------------------|-------|-------|-------|-------|--------|
|                   | 20    | 50    | 100   | 200   | random |
| Early burst       | 0.910 | 0.930 | 0.926 | 0.906 | 0.792  |
| Recent extinction | 0.916 | 0.897 | 0.858 | 0.811 | 0.890  |

Table 4: Proportion of points from the LTT plots falling below the predicted LTT line. See Table 3 for details.

| Model             | $N$   |       |       |       |        |
|-------------------|-------|-------|-------|-------|--------|
|                   | 20    | 50    | 100   | 200   | random |
| Early burst       | 0.353 | 0.358 | 0.343 | 0.310 | 0.716  |
| Recent extinction | 0.278 | 0.276 | 0.257 | 0.233 | 0.616  |

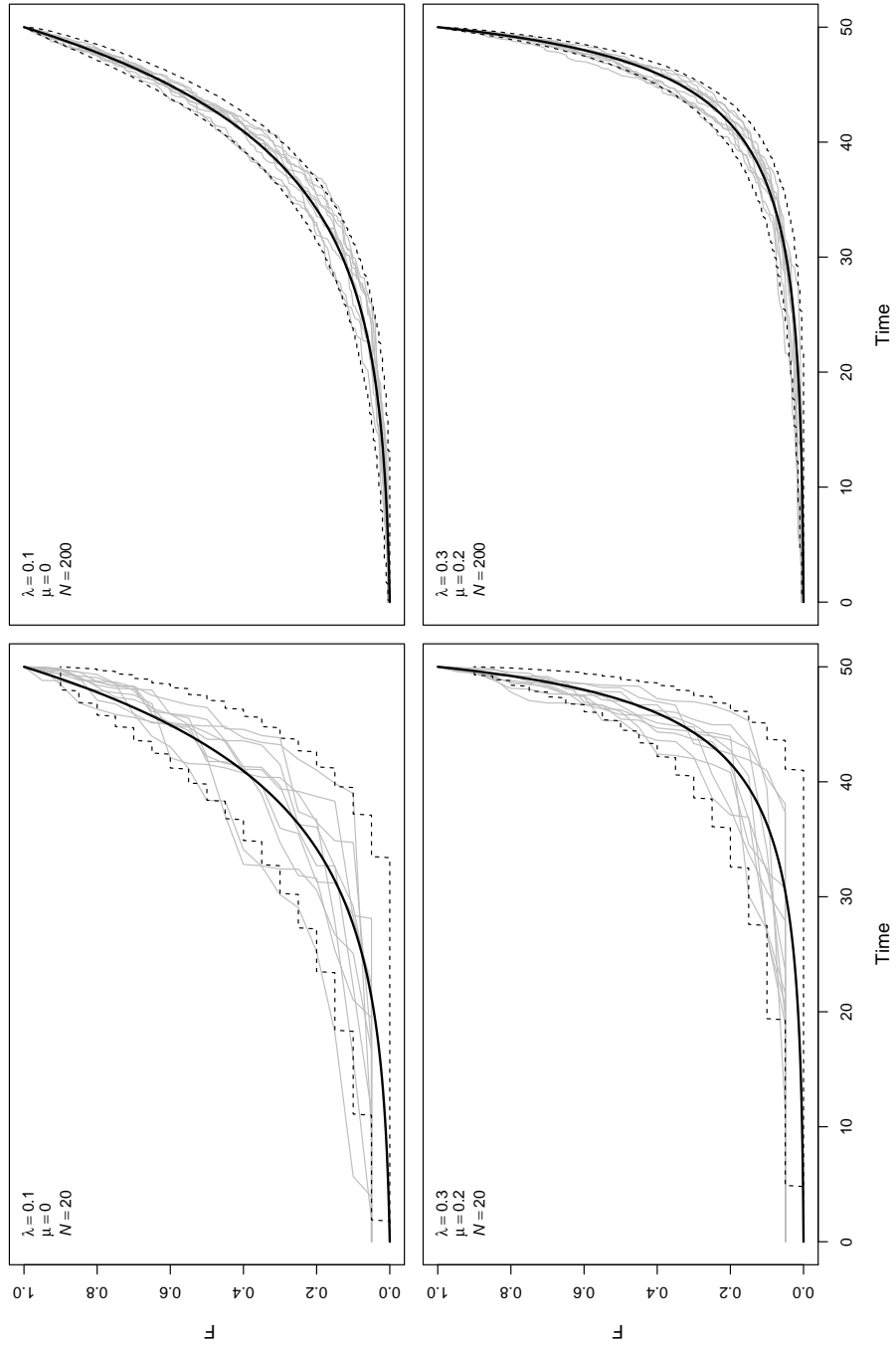
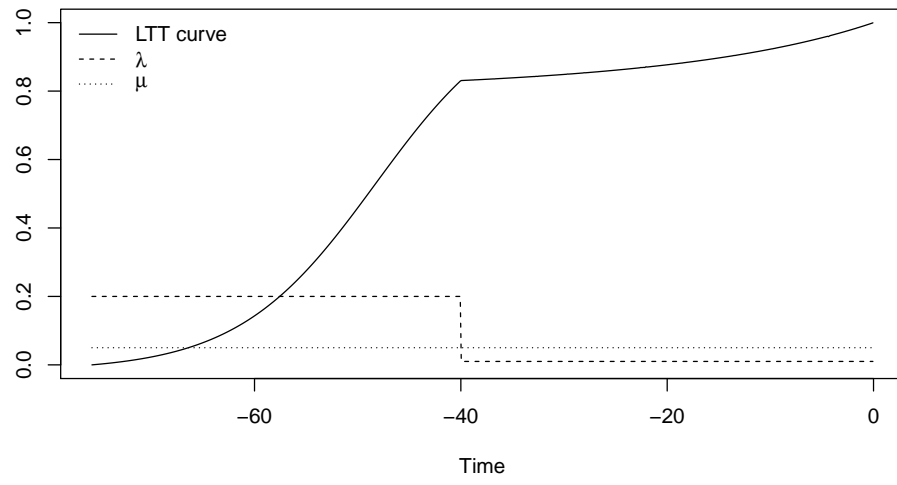


Figure 1: Lineage-through time plots for ten simulated trees with different values of speciation ( $\lambda$ ) and extinction ( $\mu$ ) rates and tree size ( $N$ ). The thick line shows the predicted LTT distribution, and the dashed lines delimit the 95% prediction intervals. The y-axes are scaled to one. F: cumulative proportions of lineages.

(a)



(b)

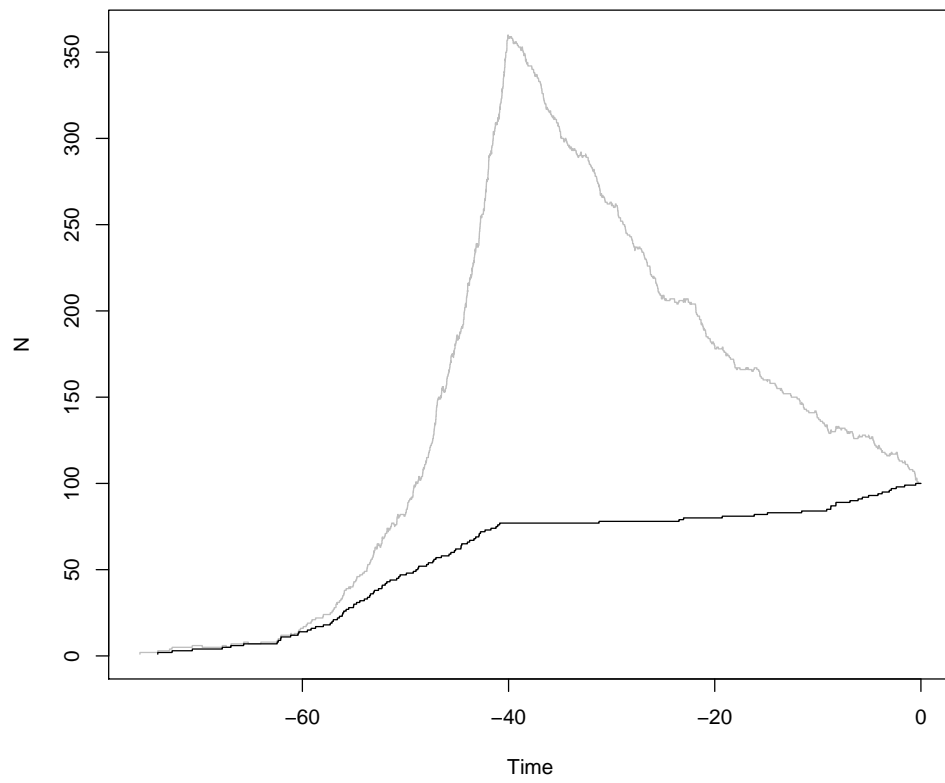


Figure 2: (a) The early burst model of speciation showing the parameters ( $\lambda$  and  $\mu$ ) and the predicted LTT curve. (b) The LTT plot from a phylogeny simulated with this model (black line) and the number of living lineages (grey line) from the same simulation.



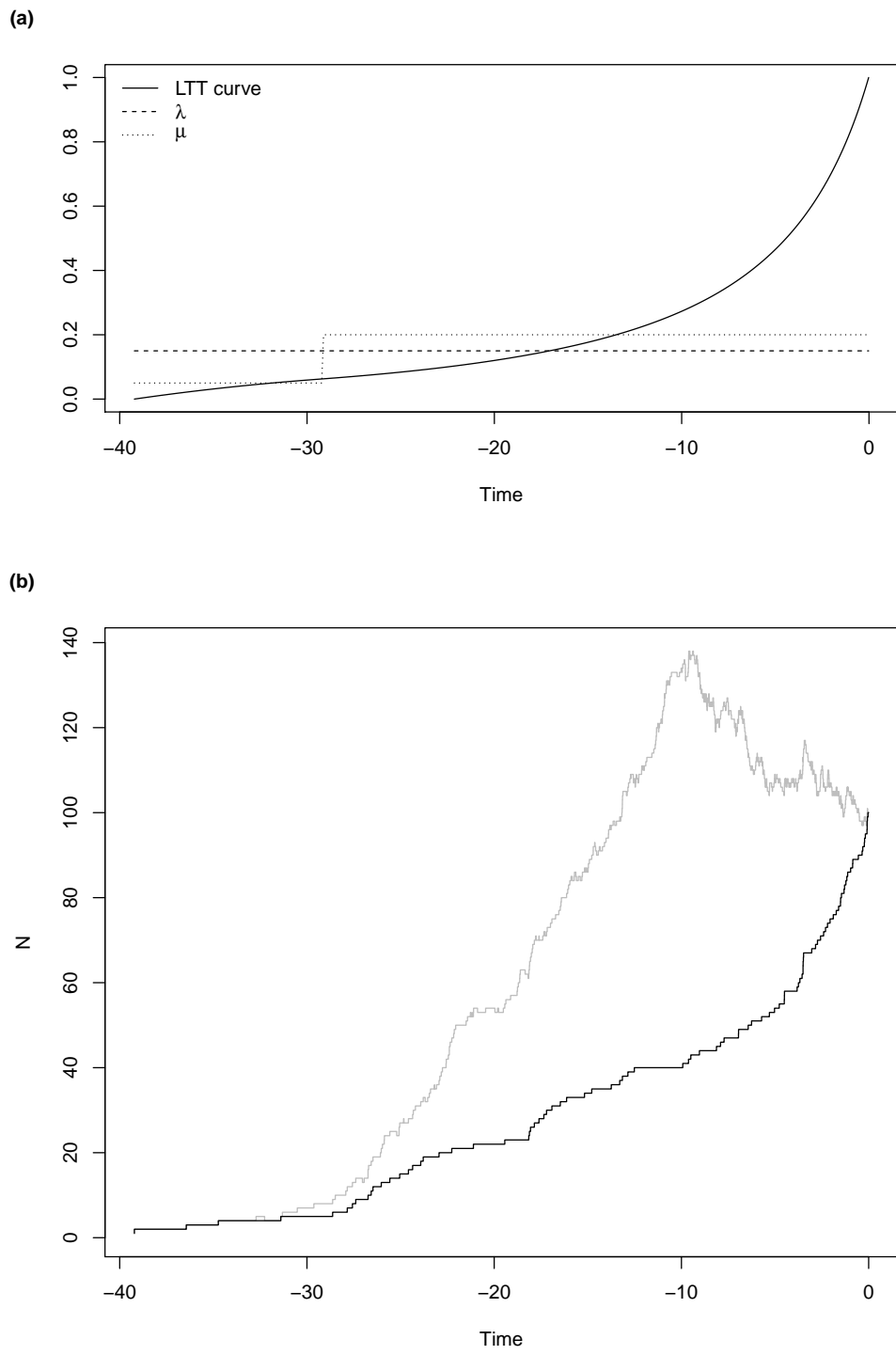


Figure 3: (a) A model of increasing extinction in recent time showing the parameters ( $\lambda$  and  $\mu$ ) and the predicted LTT curve. (b) The LTT plot from a phylogeny simulated with this model (black line) and the number of living lineages (grey line) from the same simulation.